ADVANCED FUNCTIONAL MATERIALS
www.afm-journal.de

Materials Views
www.MaterialsViews.com

Nafion–Carbon Nanocomposite Membranes Prepared Using Hydrothermal Carbonization for Proton-Exchange-Membrane Fuel Cells

By *Zhanli Chai, Cheng Wang,* Hongjie Zhang, Cara M. Doherty, Bradley P. Ladewig, Anita J. Hill,* and *Huanting Wang**

Nafion–carbon (NC) composite membranes were prepared by hydrothermal treatment of Nafion membrane impregnated with glucose solution. The carbon loading of the NC membrane was tuned by controlling the hydrothermal carbonization time. X-ray diffraction, Fourier-transform infrared spectroscopy, scanning electron microscopy, thermogravimetric analysis, and positron annihilation lifetime spectroscopy were used to characterize plain Nafion and NC composite membranes. Nafion–carbon composite membranes exhibited better proton conductivity and reduced methanol permeability than those of the plain Nafion membrane. A single cell prepared with the NC composite membrane with a carbon loading of 3.6 wt% exhibited the highest cell performance. Compared with the cell performance of plain Nafion membrane, the maximum power density of the new cell improved by 31.7% for an H_2/O_2 fuel cell at room temperature, and by 44.0% for a direct methanol fuel cell at 60 °C.

1. Introduction

Proton-exchange-membrane fuel cells (PEMFCs) have attracted much attention as a clean energy source because of their high energy density and efficiency, with low emissions, for various applications such as electric vehicles, portable electronics, and residential power generation.[1–7] Up to now, polyperfluorosulfonic acid ionomer (e.g. Nafion) based membranes are the most widely used proton-exchange membrane for PEMFCs due to their excellent chemical, mechanical, and thermal stability, and high proton conductivity. Nafion consists of a polytetrafluoroethylene backbone and perfluorinated vinyl ether pendant side chains terminated by an ionic sulfonate group. Because of this amphiphilic composition, a nanophase separation occurs between the hydrophobic matrix and hydrophilic ionic domains in hydrated Nafion.[5] Therefore, such a membrane must be fully hydrated for good proton conductivity. Nafion-based membranes have high fuel (especially methanol) permeability, commonly referred to methanol crossover, because methanol easily transports with the solvated protons through the water.[7]

Significant efforts have been made to improve the performance of Nafion membranes by incorporating other materials as fillers. Many materials, including silicon oxide,[8–12] titania,[13,14] zirconia,[15] zirconium phosphates,[16] Pd,[17] zeolites,[18] carbon nanotube,[19,20] montmorillonite,[21] and poly(furfuryl alcohol)[22] have been used as fillers to form Nafion-based composite membranes. The incorporation of these fillers was achieved via either mixing Nafion solution/melt with fillers or their precursors followed by casting,[10–15,19–21] or infiltrating fillers or their precursors into commercial Nafion membranes.[8–9,16–18,22] These composite membranes often show low methanol permeability but undesirable reduction in proton conductivity. This reduction is because many filler materials either have no proton conductivity or are less proton conductive than the plain Nafion membrane, and they occupy the hydrophilic channels of the Nafion membrane, which results in decreased proton conductivity and methanol crossover.[18,19] The introduction of filler particles may also reduce the flexibility and mechanical strength of the membrane, partially caused by their inhomogeneous distribution within the Nafion matrix. To improve the proton conductivity and uniformity of Nafion composite membranes, fillers with acidic groups such as sulfonic acid ($-SO_3H$), superacid, and carboxylic acid (–COOH) have been incorporated using a sol solution of filler materials.[12,15,19] The development of new methods to improve the performance of Nafion membranes in PEMFCs still remains an interesting topic of research.

[*] Prof. C. Wang, Prof. H. J. Zhang
State Key Laboratory of Rare Earth Resource Utilization
Changchun Institute of Applied Chemistry
Chinese Academy of Sciences
Changchun 130022, P. R. China
E-mail: cwang@ciac.jl.cn
Dr. Z. L. Chai, Dr. B. P. Ladewig, Prof. H. T. Wang
Department of Chemical Engineering
Monash University
Clayton VIC 3182, Australia
E-mail: huanting.wang@eng.monash.edu.au
Dr. Z. L. Chai
College of Chemistry and Chemical Engineering
Inner Mongolia University
Inner Mongolia 010021, P. R. China
Dr. C. M. Doherty, Dr. A. J. Hill
CSIRO Materials Science and Engineering
Locked Bag 33, Clayton South MDC, VIC 3169, Australia

DOI: 10.1002/adfm.201001412

Herein, we report a novel method for the modification of Nafion membrane by forming Nafion–carbon (NC) composite membranes via hydrothermal carbonization. Hydrothermal carbonization has been shown to be a promising process to produce carbon nanoparticles from carbohydrates such as glucose.[23–26] These carbon nanoparticles have a unique structure, consisting of a carbon core and a hydrophilic shell with functional groups such as –COOH and –OH. The hydrophilic shells mainly originate from aromatic compounds and oligosaccharides, which are the intermediates of the condensation of glucose during the hydrothermal process. So far, there has been no report on the modification of Nafion membrane using amorphous carbon species, including carbon prepared via hydrothermal carbonization. In principle, the presence of impermeable carbon nanoparticles uniformly distributed in Nafion matrix should help to reduce methanol permeation through the composite membranes. Because of their hydrophilic surfaces, the carbon nanoparticles are compatible with the hydrophilic channels of Nafion membranes, and thus have less influence on proton conduction than do hydrophobic polymer fillers such as crosslinked poly(furfuryl alcohol).[22] In the present work, glucose was used as a carbon precursor to modify commercial Nafion membranes, and carbonaceous networks were then produced inside the Nafion membrane under hydrothermal conditions. By controlling the reaction time, the carbon loading in NC composite membranes can be readily tuned. Our experimental results show that NC composite membranes have higher proton conductivity and lower methanol permeability than the plain Nafion membrane. The composite membranes exhibited significantly improved performance in PEMFCs compared with that of the plain Nafion membrane.

2. Results and Discussion

The appearance of the Nafion membrane changed after carbon incorporation. The pure Nafion 117 membrane is transparent, and the color of the NC composite membrane changes from brownish to black as the carbon loading increases from 1.5 to 9.8 wt%. The X-ray diffraction (XRD) patterns of pure Nafion membrane and NC composite membranes with different carbon loading are shown in **Figure 1**. There are two characteristic broad peaks at 17° and 40° observed for pure Nafion 117 membrane.[18] As the carbon loading increases from 1.5 to 9.8 wt%, the intensities of these two peaks drop, which indicates a progressive decrease of the crystallinity of Nafion matrix. Meanwhile a broad peak at around 23° arises from the glucose-derived carbon in NC composite membranes,[29] and its intensity increases with increasing carbon loading.

The Fourier-transform infrared (FTIR) spectra of plain Nafion and NC composite membranes are displayed in **Figure 2**. The major vibrational bands associated with the plain Nafion membrane are found in all NC composite membrane samples. The C–F stretching vibrations of the polytetrafluoroethylene (PTFE) backbone can be observed between 1000 and 1400 cm^{-1}. The bands at 1057 and 980 cm^{-1} are attributed to the stretching vibrations of SO_3^- and C–O–C of Nafion, respectively.[10] In NC composite membranes, four main peaks at 3100–3700, 2920, 1700, and 1620 cm^{-1}, which are ascribed to the stretching of O–H, H–C=O, C=O, and H–O–H, respectively, arise from the glucose-derived carbon.[24] On comparison of NC composite membranes with plain Nafion membrane, the characteristic vibrations of Nafion are weakened in NC composite membranes; as expected, with increased the carbon loading the broad peak in the range of 3100–3700 cm^{-1} becomes broader and stronger, and the three peaks at 2918, 1701, and 1620 cm^{-1} become more intense.

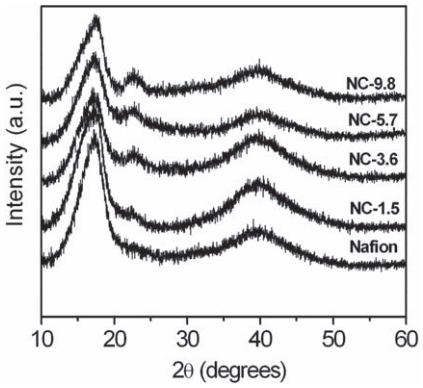

Figure 1. XRD patterns of Nafion 117 membrane and NC composite membranes with different carbon loadings. NC-1.5: 1.5 wt% carbon, NC-3.6: 3.6 wt% carbon, NC-5.7: 5.7 wt% carbon, and NC-9.8: 9.8 wt% carbon.

Figure 3 shows the scanning electron microscopy (SEM) images of the surface of the pristine and composite NC membranes. Similar to the plain Nafion membrane (Figure 3a), the NC-1.5 membrane exhibits a smooth surface (Figure 3b) and no carbon particles are visible on its surface. When the carbon loading increases to 3.6 wt%, the surface of the NC composite membrane (NC-3.6) becomes rough, but there are still no particles observed on the surface (Figure 3c). Uniformly distributed carbon nanoparticles are seen on the surface of NC-5.7 membrane (Figure 3d). These carbon nanoparticles are partially embedded inside the Nafion matrix, as the carbon nanoparticles remain on the surface of the composite membrane after vigorous postsynthesis treatment with 1 M sulfuric acid solution at 80 °C for 1 h in conjunction with ultrasonication. The Nafion

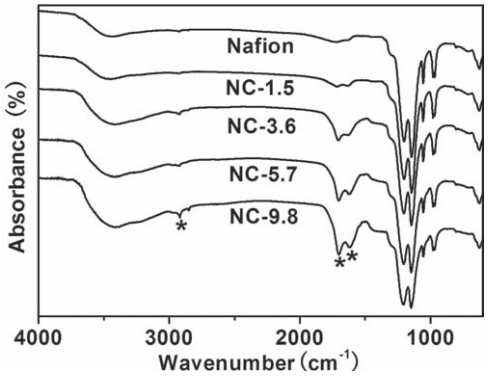

Figure 2. FTIR spectra of pure Nafion 117 membrane and NC composite membranes with different carbon loadings.

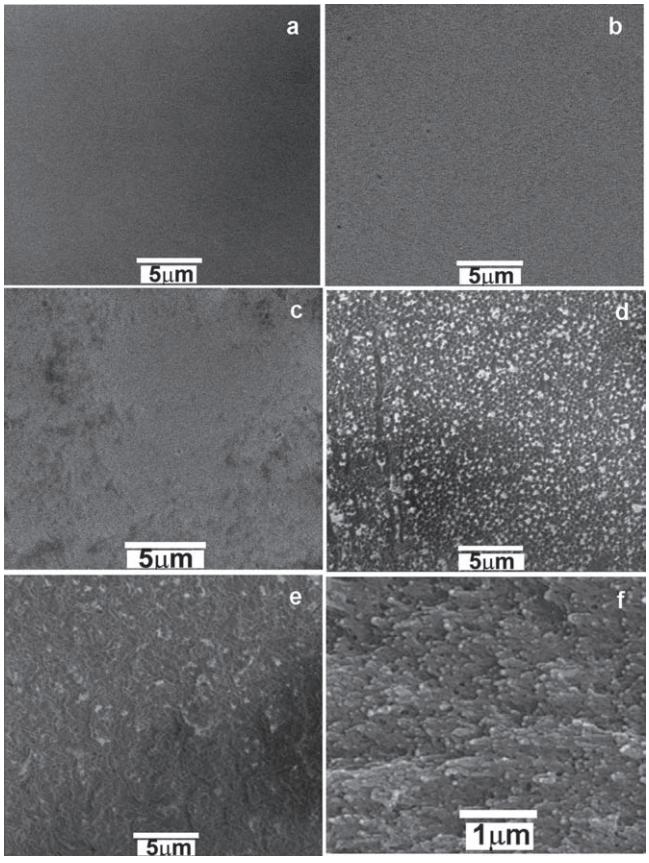

Figure 3. SEM images of the surfaces of plain Nafion and NC composite membranes with different carbon loadings. a) Nafion 117 membrane, b) NC-1.5, c) NC-3.6, d) NC-5.7, e) NC-9.8, and f) SEM image of cross-sectional NC-9.8 composite membrane.

structure is then further swollen after the carbon loading is increased to 9.8 wt%. The NC-9.8 membrane shows a rough surface texture with fewer particles exposed (Figure 3e). As shown in the cross-sectional SEM image in Figure 3f, carbon nanoparticles are uniformly distributed throughout the NC-9.8 membrane.

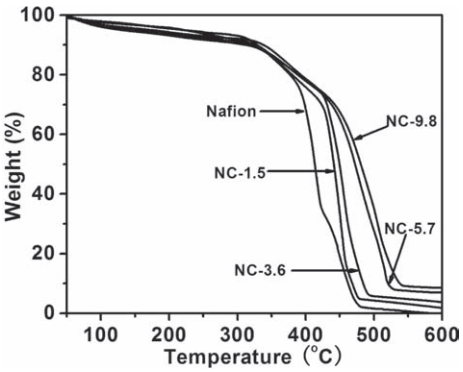

Figure 4. TGA curves of plain Nafion 117 membrane and NC composite membranes with different carbon loadings.

Thermal analysis was used to determine the degradation temperature and carbon loading of the membranes. **Figure 4** shows the thermogravimetric analysis (TGA) results of the Nafion and NC composite membranes. The small weight loss from 30–320 °C for all the membranes can be attributed mainly to loss of residual water within the membrane. According to the literature,[30] the weight loss in the temperature range of 320–550 °C for plain Nafion membrane reflects that the decomposition of Nafion occurs in at least three stages. The first stage (320 °C–410 °C) is associated with the desulfonation process while the second stage (410 °C–470 °C) and the third stage (470–550 °C) may be related to side-chain and PTFE-backbone decomposition, respectively. The NC composite membranes show a smaller weight loss between 320–550 °C (i.e., 87.5% for NC-1.5, 85.4% for NC-3.6, 82.3% for NC-5.7, and 80.2% for NC-9.8) than plain Nafion membrane (89.0%), which shows that the carbon loading increases from NC-1.5 to NC-9.8 due to the higher thermal stability of carbon nanopaticles than of the Nafion matrix. Moreover, the differences in weight losses between the plain Nafion membrane and the NC composite membranes in the TGA curves are regarded as the carbon loadings in NC membranes, which are close to the weight change of the membranes before and after carbon incorporation.

Table 1. PALS results for Nafion and NC composite membranes under dry and 100% RH conditions.

Sample	Testing conditions	o-Ps lifetime, τ_3 [ns]	o-Ps intensity, I_3 [%]	Free-volume-element radius [Å] ±0.03	Free-volume-element volume [Å^3] ±4
Nafion	dry	3.204 ± 0.04	7.848 ± 0.09	3.77	224
NC-1.5 (1.5 wt% C)	dry	3.197 ± 0.05	7.646 ± 0.07	3.77	224
NC-3.6 (3.6 wt% C)	dry	3.093 ± 0.03	7.472 ± 0.08	3.70	212
NC-5.7 (5.7 wt% C)	dry	3.063 ± 0.04	6.145 ± 0.10	3.68	209
Nafion	100% RH	2.822 ± 0.02	10.283 ± 0.14	3.51	181
NC-1.5	100% RH	2.827 ± 0.02	10.422 ± 0.04	3.52	183
NC-3.6	100% RH	2.770 ± 0.03	10.309 ± 0.07	3.48	177
NC-5.7	100% RH	2.812 ± 0.04	8.568 ± 0.08	3.51	181

The PALS results are summarized in **Table 1**. Under dry conditions, there was no obvious difference observed between the Nafion membrane and the NC membrane with a small carbon loading (e.g., 1.5 wt%); the ortho positronium (o-Ps) lifetime (τ_3) and intensity (I_3) and free volume element size of the membrane decreased with increased carbon loading. This result indicates that the incorporation of carbon has led to a reduction in the free volume of Nafion. After the membranes were fully hydrated, the lifetime decreased by approximately 0.34–0.49 ns. This reduction in lifetime indicates that the water is filling the free-volume elements of the membrane and reducing their size. In the meantime, the intensity increased significantly, which indicates an increase in the

free-volume concentration from the swelling of the polymer. There was a drop of approximately 0.05 nm in free-volume-element diameter between the dry and 100% relative humidity (RH) samples. As previously suggested in the literature, the free-volume elements are present in the interfacial region among the cluster, filler, and hydrophobic backbone. After swelling due to moisture, these free-volume elements reduce in size.[31] There is a significant drop in the intensity for dry and hydrated NC-5.7 as compared to all other membranes, which indicates a reduction of free-volume concentration at that filler loading. Comparison of the dry and hydrated free-volume response between plain Nafion and the NC samples is informative. Although carbon loading is shown to alter the dry-membrane free volume, carbon loading still allows the membrane free-volume elements to respond to hydration similarly to plain Nafion. Such structure changes in the hydrated samples should affect the properties (e.g., proton conductivity and methanol permeability) of the membranes as discussed below.

Table 2 lists the thickness and water uptake of plain Nafion and NC composite membranes with different carbon loadings. As the carbon loading increases, the membrane thickness gradually increases from 178 μm for plain Nafion to 285 μm for NC-9.8; in other words, it increases by 15.7%, 24.2%, 37.0%, and 60.1% for NC-1.5, NC-3.6, NC-5.7, and NC-9.8, respectively. The water uptake of pure Nafion membrane is 38 wt%, which is comparable to that reported in the literature.[10] The water uptake of the membrane is substantially enhanced with increased carbon loading, and this effect is related to the hygroscopic properties of the glucose-derived carbon.

The proton conductivity and methanol permeability of plain Nafion 117 and NC composite membranes are shown in **Figure 5**. The proton conductivity of the membrane initially increases and reaches its maximum (0.126 S cm^{-1}) at 3.6 wt% carbon loading, and then drops slightly when the carbon loading further increases (e.g. 5.7 and 9.8 wt%). These drops of NC-5.7 and NC-9.8 are presumably caused by their much bigger thickness than the NC membranes with lower carbon loadings, which could be seen from Table 2, and a slightly increased free volume in their hydrated states, which was revealed by PALS. Moreover, the proton conductivities of the composite membranes are all higher than that of the pure Nafion membrane, which indicates that the incorporation of hydrophilic carbon nanoparticles alters the structure of the Nafion matrix and assists in proton conductivity. On the other hand, the methanol permeability of the membrane decreases continuously with increased carbon loading; this indicates that, like many other filler materials, the carbon nanoparticles effectively reduce methanol crossover. As shown in Figure 5, NC-9.8 membrane possesses the lowest methanol permeability of 3.6×10^{-7} cm^2 s^{-1} which is about six times less than that of plain Nafion membrane (2.3×10^{-6} cm^2 s^{-1}). The reduced methanol permeability of the composite membranes might partially arise from the increase in membrane thickness after carbon incorporation.

Table 2. Thickness and water uptake capacity of plain Nafion and NC membranes measured at room temperature.

Sample	Carbon loading [wt%]	Thickness [μm]	Water uptake [wt%]
Nafion	0	178	38.0
NC-1.5	1.5	206	44.4
NC-3.6	3.6	221	51.7
NC-5.7	5.7	244	59.1
NC-9.8	9.8	285	70.6

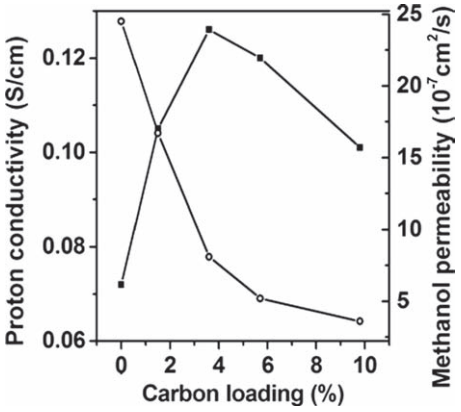

Figure 5. Proton conductivity and methanol permeability of plain Nafion 117 and NC composite membranes with different carbon loadings.

The cell performances of the pure Nafion 117 membrane and NC composite membranes tested in the operation of a single cell with H_2/O_2 at room temperature and with methanol/O_2 (DMFC) at 60 °C are shown in **Figure 6**. In the case of the H_2/O_2 fuel cell (Figure 6a), the open-cell voltage (OCV) of the cell made with NC composite membranes is slightly higher than that of the cell with the plain Nafion 117 membrane. NC-1.5 and NC-3.6 perform better than the plain Nafion membrane whereas NC-5.7 and NC-9.8 show poorer performance than Nafion; their maximum current density is in the order of NC-3.6 > NC-1.5 > Nafion > NC-5.7 > NC-9.8. Specifically, the cell with the NC-3.6 membrane exhibits the highest power density (92.1 mW cm^{-2}) and a 31.7% improvement in peak power density as compared with that of Nafion. The cell performance of DMFCs at 60 °C is shown in Figure 6b. Similarly, the NC-3.6 composite membrane shows the best performance of all five membranes. The OCVs of the cells made with these membranes are in the order of NC-3.6 (0.69 V) > NC-1.5 (0.67 V) > Nafion (0.64 V) > NC-5.7 (0.60 V) > NC-9.8 (0.53 V). The peak power density of the cell with the NC-3.6 membrane is 36.3 mW cm^{-2}, which is 44.0% higher than the cell with the Nafion membrane. The highest performance observed for NC-3.6 can be explained by the following: i) NC-3.6 exhibits the highest proton conductivity and a much reduced methanol permeability; ii) NC-3.6 has a rougher surface than the plain Nafion membrane, but there are no carbon nanoparticles observed in this membrane. A better contact (lower interfacial resistance) between the membrane and the electrodes can be achieved for NC-3.6. By contrast, the NC composite membranes with higher carbon loadings (5.7% and 9.8%) would result in much higher interfacial resistance between the membrane and the electrodes, and thus lower cell performance.

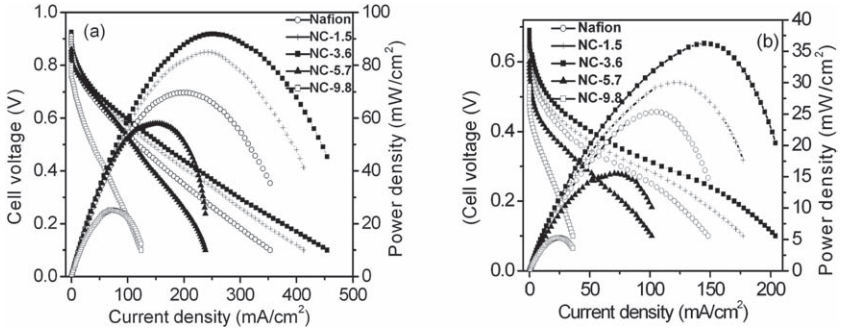

Figure 6. Cell performance of plain Nafion membrane and NC membranes with different carbon loadings. a) H_2/O_2 cell performance at room temperature, b) cell performance of DMFC cell operated at 60 °C and fed with 2 M methanol.

3. Conclusions

Nafion–carbon composite membranes were fabricated by incorporating carbon into Nafion membranes via the hydrothermal carbonization method. The carbon loading could be controlled by the hydrothermal treatment conditions such as reaction time. Our study showed that NC composite membranes had improved proton conductivity compared with the plain Nafion membrane, and the composite membrane with a carbon loading of 3.6 wt% possessed the highest proton conductivity. Meanwhile, the methanol permeability of the composite membranes dropped substantially with increased carbon loading. These results could be attributed to structural change in the composite membranes due to the incorporation of carbon particles. The performance of the cells made with NC composite membranes with lower carbon coatings (e.g. 1.5 and 3.6 wt%) was significantly enhanced. This work offers a new and simple method for modifying a Nafion membrane to improve its fuel-cell performance.

4. Experimental Section

Preparation of Nafion–Carbon (NC) Composite Membranes: In a typical synthesis, a 2 cm × 2 cm piece of Nafion 117 membrane (Sigma–Aldrich) was pretreated by using a standard procedure, i.e. in 3.0 wt% H_2O_2 solution at 80 °C for 1 h, 1.0 M H_2SO_4 solution at 80 °C for 1 h, and distilled water at 80 °C for 1 h. Then, the membrane was further swollen in a boiling methanol–water solution (1:1 (v/v)). 20.0 mL of 5.0 wt% glucose aqueous solution was loaded in a Teflon-lined stainless-steel autoclave with a volume of 60 mL, and then the swollen Nafion 117 membrane was immersed in the glucose solution. After hydrothermal treatment at 190 °C for 1–4 h, the resultant NC membranes were treated with the same standard procedure as described above. The carbon loadings of the NC membranes were determined by TGA, which was confirmed by weighing the dry Nafion membrane sample before and after hydrothermal carbonization process; the NC membranes treated for 1, 2, 3, and 4 h contained ca. 1.5, 3.6, 5.7, and 9.8 wt%, and are denoted as NC-1.5, NC-3.6, NC-5.7, and NC-9.8, respectively.

Material Characterization: Powder XRD patterns of the dried membranes were recorded on a Bruker D8 Focus diffractometer with Cu Kα radiation and a Linux detector at a scanning rate of 2° min^{-1} in the 2θ range of 10°to 70°. Field-emission scanning electron microscopic (FE-SEM) images were obtained with a Hitachi S-4800 microscope operated at an acceleration voltage of 10 kV. FTIR spectra were measured with a Vertex 70 FTIR spectrophotometer (Bruker) equipped with an MTEC (model 300) photoacoustic cell. TGA was conducted using a Pyris Diamond thermal analyzer in the range of 25–600 °C at a heating rate of 10 °C min^{-1}. The thickness of the membranes was measured by a Contracer CV-3100/4100 instrument at room temperature.

Positron annihilation lifetime spectroscopy (PALS) was used to characterize Nafion and NC composite membranes using an automated EG&G Ortec fast-fast coincidence system with a resolution function of 250 ps at full-width half maximum (FWHM).[6] The ^{22}NaCl positron source was sealed between 2.54 μm Mylar films and required a source correction of 3.5% intensity at 1.795 ns. The membranes were cut into 1 cm^2 pieces and stacked together to ensure the membranes on each side of the source were 2 mm thick. The samples were initially analyzed dry and then soaked in water for 24 h prior to the second analysis at 100% relative humidity (RH). The films were placed on each side of the source, wrapped in Al foil and sealed in a plastic bag to prevent moisture loss and then measured so as to maintain hydration at 100% RH. At least five spectra of 1 million integrated counts were collected for each sample and the data were analyzed using the PFPOSFIT program. The PALS parameters for the membranes did not change as a function of contact time with the source. Three lifetimes were fitted with the shortest, τ_1 fixed at 125 ps, characteristic of para positronium (p-Ps) self-annihilation. The relationship between the ortho positronium (o-Ps) lifetime τ_3 and the free volume element radius was calculated using the Tao–Eldrup model.[27,28]

Measurement of Water Uptake, Proton Conductivity and Methanol Permeability: The water uptake (w.u.%) measurement gives information on the water retention of the membrane and it is calculated from the difference in weight between wet and dry samples. The wet weight (m_{wet}) was determined after immersing the sample in water at room temperature for 48 h while, for the dry weight (m_{dry}), the sample was kept in an oven at 80 °C under vacuum for 10 h. The percentage of water uptake is given by

$$\text{w.u.\%} = \left[\frac{m_{wet} - m_{dry}}{m_{dry}}\right] \times 100. \quad (1)$$

Proton conductivity of the plain and NC composite membranes was measured using the four-electrode AC impedance method in the frequency range of 0.1 Hz to 100 kHz, and at 10mV AC perturbation and 0.0V DC rest voltage. Impedance spectra were recorded using a Princeton Applied Research Model 273A Potentiostat (Model 5210 Frequency Response Detector, EG&G PARC, Princeton, NJ). The membranes were fixed in a measuring cell made of two outer gold wires to feed current to the sample and two inner gold wires to measure the voltage drops. Conductivity measurements under fully hydrated conditions were carried out with the cell immersed in liquid water. The proton conductivity (σ) of the membranes was calculated using the following equation:

$$\sigma = \frac{L}{RA} \quad (2)$$

where L, R, and A denote the distance between the two inner gold wires, the resistance of the membrane, and the cross-sectional area of the membrane, respectively.

Methanol permeability of the membrane was determined using a glass diffusion cell. This glass cell consisted of two compartments, approximately 100.0 mL each; one compartment of the cell was filled with 2.0 M methanol solution, and the other with deionized water. The membrane with an effective area of 4.5 cm^2 was clamped between the two compartments, which were kept under stirring during the experiment. The methanol concentration in the receiving compartment was measured versus time using a gas chromatograph (Shimazu GC-14B) equipped with a thermal-conductivity detector.

The methanol permeability (P) was calculated using the following equation:

$$C_B(t) = \frac{AP}{V_B L} C_A (t - t_0) \quad (3)$$

where $C_B(t)$ is the methanol concentration measured in the receiving compartment as a function of time, V_B the volume of receiving compartment, and L and A are the thickness and effective area of membrane, respectively. P is the methanol permeability and can be determined from the slope of the plot of methanol concentration in the receiving compartment versus time.

Single Fuel-Cell Performance: Gas-diffusion electrodes were prepared by brushing PtRu/C catalyst (20 wt%, E-TEK) onto carbon paper (Toray TGPH-090, E-TEK). After the desired amount of Pt loading (8.0 mg cm^{-2}) was achieved, a thin layer of 8 wt% Nafion solution was sprayed onto the surface of each electrode (1.0 mg Nafion cm^{-2}). Then the pretreated Nafion 117 membrane or carbon composite membrane was sandwiched between the two gas-diffusion electrodes, and hot-pressed into a membrane elctrode assembly (MEA; 1.25 cm^2) at 25 MPa and 140 °C for 5 min. The anode and cathode sections were connected with thin silver wires. The prepared MEA was mounted in a single cell holder composed of ribbed channels for supplying gases or methanol. H_2/O_2 fuel cell tests were performed at room temperature and an RH value of 30% at 1 atm of pressure, and flow rates of hydrogen and oxygen of 30–50 mL min^{-1}. For the direct-methanol fuel-cell system, the test was undertaken at an operating temperature of 60 °C with 2.0 M methanol aqueous solution as the fuel. The flow rate of oxygen was also 30–50 mL min^{-1} for the cathode side. The current–voltage (I–V) and current–power density (I–P) curves of the cell were plotted from the data recorded on a DC electronic load (IT8511, ITECH Electronic Co., Ltd.).

Acknowledgements

The authors are grateful for the financial support from NSFC (20671087) and the National Basic Research Program of China (2007CB925101), and the Australian Research Council (ARC). Z.C. thanks the Department of Chemical Engineering at Monash University for supporting her visiting study.

Received: July 14, 2010
Published online: October 1, 2010

[1] R. Devanathan, *Energy Environ. Sci.* **2008**, *1*, 101
[2] M. A. Hickner, H. Ghassemi, Y. S. Kim, B. R. Einsla, J. E. McGrath, *Chem. Rev.* **2004**, *104*, 4587.
[3] P. Costamagna, S. Srinivasan, *J. Power Sources* **2001**, *102*, 242.
[4] G. Gebel, *Polymer* **2000**, *41*, 5829.
[5] J. Y. Kim, W. C. Choi, S. I. Woo, W. H. Hong, *J. Membr. Sci.* **2004**, *238*, 213.
[6] Q. F. Li, R. H. He, J. O. Jensen, N. J. Bjerrum, *Chem. Mater.* **2003**, *15*, 4896.
[7] A. Heinzel, V. M. Barragan, *J. Power Sources* **1999**, *84*, 70.
[8] B. P. Ladewig, R. B. Knott, A. J. Hill, J. D. Riches, J. W. White, D. J. Martin, J. C. Diniz da Costa, G. Q. Lu, *Chem. Mater.* **2007**, *19*, 2372.
[9] B. P. Ladewig, R. B. Knott, D. J. Martin, J. C. Diniz da Costa, G. Q. Lu, *Electrochem. Commun.* **2007**, *9*, 781.
[10] F. Pereira, K. Vallé, P. Belleville, A. Morin, S. Lamberts, C. Sanchez, *Chem. Mater.* **2008**, *20*, 1710.
[11] H. L. Tang, M. Pan, *J. Phys. Chem. C* **2008**, *112*, 11556.
[12] H. T. Wang, H. T. Wang, B. A. Holmberg, Z. B. Wang, L. M. Huang, A. Mitra, J. M. Norbeck, Y. S. Yan, *J. Mater. Chem.* **2002**, *12*, 834.
[13] K. T. Adjemian, R. Dominey, L. Krishnan, H. Ota, P. Majsztrik, T. Zhang, J. Mann, B. Kirby, L. Gatto, M. Velo-Simpson, J. Leahy, S. Srimvasan, J. B. Benziger, A. B. Bocarsly, *Chem. Mater.* **2006**, *18*, 2238.
[14] A. Saccà, A. Carbone, E. Passalacqua, A. D'Epifanio, S. Licoccia, E. Traversa, E. Sala, F. Traini, R. Ornelas, *J. Power Sources* **2005**, *152*, 16.
[15] M. Navarra, F. Croce, B. Scrosati, *J. Mater. Chem.* **2007**, *17*, 3210.
[16] M. Casciola, D. Capitani, A. Comite, A. Donnadio, V. Frittella, M. Pica, M. Sganappa, A. Varzi, *Fuel Cells* **2008**, *8*, 217.
[17] F. Li, P. Bertoncello, I. Ciani, G. Mantovani, P. R. Unwin, *Adv. Funct. Mater.* **2008**, *18*, 1685.
[18] Z. Chen, B. Holmberg, W. Li, X. Wang, W. Deng, R. Munoz, Y. S. Yan, *Chem. Mater.* **2006**, *18*, 5669.
[19] J. M. Thomassin, J. Kollar, G. Caldarella, A. Germain, R. Jeromea, C. Detrembleur, *J. Membr. Sci.* **2007**, *303*, 252.
[20] Y.-L. Liu, Y. H. Su, C.-M. Chang, Suryani, D.-M. Wang, J.-Y. Lai, *J. Mater. Chem.*, **2010**, *20*, 4409.
[21] C. H. Rhee, H. K. Kim, H. Chang, J. S. Lee, *Chem. Mater.* **2005**, *17*, 1691.
[22] J. Liu, H. T. Wang, S. A. Cheng, K.-Y. Chan, *J. Membr. Sci.* **2005**, *246*, 95.
[23] Y. Shin, L.-Q. Wang, I.-T. Bae, B. W. Arey, G. J. Exarhos, *J. Phys. Chem. C* **2008**, *112*, 14236.
[24] X. Sun, Y. Li, *Angew. Chem. Int. Ed.* **2004**, *43*, 597.
[25] M.-M. Titirici, A. Thomas, M. Antonietti, *J. Mater. Chem.* **2007**, *17*, 3412.
[26] Q. Wang, H. Li, L. Chen, X. Huang, *Carbon* **2001**, *39*, 2211.
[27] S. J. Tao, *J. Chem. Phys.* **1972**, *56*, 5499.
[28] M. Eldrup, D. Lightbody, J. N. Sherwood, *Chem. Phys.* **1981**, *63*, 51.
[29] S. H. Lee, M. Mathews, H. Toghiani, D. O. Wipf, C. U. Pittman, *Chem. Mater.* **2009**, *21*, 2306.
[30] M. K. Mistry, N. R. Choudhury, N. K. Dutta, R. Knott, Z. Q. Shi, S. Holdcroft, *Chem. Mater.* **2008**, *20*, 6857.
[31] H. S. Sodaye, P. K. Pujari, A. Goswami, S. B. Manohar, *J. Polym. Sci. B-Polym. Phys.* **1998**, *36*, 983.